TRANSLATIONAL BAND OF GASEOUS HYDROGEN AT LOW TEMPERATURE

E. H. WISHNOW,[1,2] I. OZIER,[1] H. P. GUSH,[1] AND J. SCHAEFER[3]

ABSTRACT

A comparison is made between the observed submillimeter absorption spectrum of normal hydrogen gas at three different temperatures near 25 K and a fully quantum mechanical ab initio calculated spectrum. Measurements cover the wavenumber range 20–320 cm^{-1}, where, under the experimental conditions of low temperature and low pressure, the pure translational band is observed virtually isolated from the $S(0)$ rotational line. The theoretical analysis shows that the H_2 spectrum is primarily due to transient collision-induced dipole moments in pairs of colliding molecules, i.e., due to free-free transitions. Bound-free transitions of the H_2 dimer are responsible for an additional $\sim 10\%$ of the absorption intensity. The agreement between the theoretical spectra and the measurements is excellent, thereby verifying that the intermolecular potential, the wave functions, and the model of the induced dipole moment have all been accurately represented. As a consequence, it is possible to predict with confidence the absorption spectrum of H_2 in physical conditions not readily accessible to laboratory measurements.

Subject headings: infrared: general — methods: laboratory — methods: numerical — molecular processes

1. INTRODUCTION

It is well known that, because of its symmetry, an isolated homonuclear diatomic molecule in the electronic ground state does not have a normal rotation-vibration spectrum. However, in a colliding pair of such molecules, transient electric dipole moments modulated by the vibrational, rotational, and translational motion are induced by the intermolecular forces between the collision partners. As a result, absorption takes place where the intensity is proportional to the square of the gas density. This phenomenon is called collision-induced absorption, and its experimental study, combined with theoretical analysis, gives valuable information concerning molecular interactions (Frommhold 1993). In the case of hydrogen, collision-induced absorption has importance in the interpretation of the spectra of planetary atmospheres and can have implications for the detection of interstellar H_2 molecules.

The far-infrared spectrum of normal hydrogen in the temperature region studied here, 22–36 K, consists of three components: the $S(0)$ and $S(1)$ features of the rotational-translational band which have peaks near 360 and 590 cm^{-1}, respectively, and the much weaker pure translational band which extends from 0 to over 400 cm^{-1}. In the colliding pair of molecules, the rotational angular momentum quantum numbers of the individual monomers are labeled j_1 and j_2, while the quantum number for the rotational angular momentum of the collision complex is denoted by l. The $S(0)$ and $S(1)$ features arise from the absorption of radiation by rotational transitions of one of the interacting molecules, and by accompanying transitions between translational energy states. The dominant selection rules are Δj_1, $\Delta j_2 = \pm 2, 0$ or $0, \pm 2$, and $\Delta l = \pm 1, \pm 3$. In the pure translational band, the energy of the absorbed photon goes entirely into the colliding molecules' relative translational motion. The dominant selection rules in this case are $\Delta j_1 = \Delta j_2 = 0$ and $\Delta l = \pm 1, \pm 3$.

The spectral features are very broad as a consequence of the continuum of translational energy states, and at room temperature the H_2 rotational lines and the translational band are blended together. Because the molecules have a Maxwellian velocity distribution, the widths of the features are proportional to $T^{1/2}$, where T is the temperature. By performing measurements at temperatures near 25 K, it is possible to observe the pure translational band isolated from the $S(0)$ feature.

Under low-temperature conditions, where the translational energy kT (k is Boltzmann's constant) is of the order of the depth of the intermolecular potential, a gas sample contains a substantial number of dimers, pairs of molecules weakly bound by van der Waals forces. The lifetime of the dimers is limited by the time between molecular collisions. In addition, there exists a significant population in resonance states arising from pairs of molecules orbiting each other with energies slightly above the dissociation limit. The resonance states have lifetimes typically long compared to the collision duration but short compared to the time between collisions. The dimers possess an electric dipole moment and transitions between bound states and/or resonance states give rise to weak spectral lines (Schaefer 1994). For $\Delta j_1 = \Delta j_2 = 0$; $\Delta l \neq 0$; these lines fall at the low-frequency end of the translational band. For $\Delta j_1 = \pm 2$ or $\Delta j_2 = \pm 2$; $\Delta l \neq 0$; lines appear as satellites near the free molecule rotational lines, e.g., near 354 cm^{-1} for the $S(0)$ line. Corresponding to each of the above cases, there arise similar bound-free (and free-bound) spectral lines that are also weak but broad. These various contributions involving dimer and resonance states are superposed upon the broad free-free collision-induced spectrum discussed above. In fact, the initial motivation for the experimental work reported here was the hope of finding evidence of the dimer/resonance contributions to the translational spectrum.

In a complete theoretical treatment of the hydrogen spectrum, it is essential to take the dimer states, the orbiting resonances, and all significant continuum states into account. Furthermore, at the low temperatures studied here, quantum effects in the translational motion are important for a molecule as light as H_2. The de Broglie wave-

[1] Department of Physics and Astronomy, University of British Columbia, Vancouver, BC, V6T 1Z1, Canada.

[2] Astrophysics Group, V Division, Lawrence Livermore National Laboratory, P.O. Box 808, Livermore, CA 94551; wishnow@llnl.gov.

[3] Max-Planck-Institut für Astrophysik, Karl-Schwarzschild-Strasse 1, 85740 Garching, Germany; jas@mpa-garching.mpg.de.

length for a molecule of mass m can be written $\lambda = (h^2/2\pi mkT)^{1/2}$, where h is Planck's constant. For hydrogen at 20 K, $\lambda = 0.28$ nm. This is comparable to the intermolecular distance at the minimum in the interaction potential, namely 0.34 nm. Clearly, quantum effects must be taken fully into account, for example, in the pair distribution function. Previous comparisons have been reported of full quantum mechanical ab initio calculations and experimental measurements of the H_2 spectrum near the $S(0)$ and $S(1)$ lines at 77 K (Schaefer & McKellar 1990), and near the $S(0)$ line at 20 K (McKellar & Schaefer 1991).

A successful theoretical prediction of the translational spectrum is of considerable importance in both molecular physics and astrophysics. A comparison between the measured spectrum and the calculated spectrum, involving only the relative motion of the two H_2 molecules, can serve as a test of the intermolecular potential, the molecular wave functions and the electric dipole moment operator. It should be emphasized that the calculations carried out here involve no parameters which have been adjusted to fit these translational band experimental results.

The astrophysical applications of the comparison are both planetary and galactic. With a reliable model which takes full account of the quantum nature of the hydrogen molecules, it is possible to calculate the spectrum of the gas under physical conditions not easily attainable in the laboratory. The collision-induced spectrum of hydrogen is known to make a significant contribution to the far-infrared opacity of the giant gaseous planets; and, because of their low temperatures, the translational band is particularly important in the cases of Uranus and Neptune (Hanel et al. 1986; Conrath et al. 1989). The current theoretical model can be used in studies of the atmospheres of these giant planets by constraining the thermal opacity over the relevant ranges in temperature and pressure. This topic has been discussed recently by Birnbaum, Borysow, & Orton (1996).

It is possible that cold molecular hydrogen can make a significant contribution to the so-called missing mass of the Galaxy. Several authors have shown that rotation curves of spiral galaxies can be reproduced by models where the dark halo mass is replaced by a dark component with the same surface density as atomic hydrogen (H I) apart from a simple scaling factor (Broeils 1992, and references therein). An interesting model has been introduced by Pfenninger, Combes, & Martinet (1994) and Pfenninger & Combes (1994) in which some of the dark matter is in the form of cold molecular hydrogen gas in a realistic fractal structure with elementary fragments at densities the order of 10^9 cm^{-3}. Under assumptions discussed elsewhere (Schaefer 1997), the density of this gas can increase dramatically to the point where a portion becomes observable. The submillimeter galactic emission spectrum measured by the FIRAS-*COBE* mission (Mather et al. 1995) has been modeled (Schaefer 1996) with two contributions: cold gas (11 K) and warm dust (15–32 K). The surprising result, obtained from a large number of fits to the FIRAS spectra, is the close correlation of the H_2 column density with that of the H I (Schaefer 1996). Of particular interest here is the fact that the gas and dust model relies on a calculation of the collision-induced translational band of H_2 (in emission) at 11 K. A reliability test for this calculation is provided by the current comparison between experiment and theory for the corresponding band (in absorption) at $22 \leq T \leq 36$ K.

2. EXPERIMENTAL MEASUREMENTS

The submillimeter spectrum of normal hydrogen has been measured between 20 and 320 cm^{-1} at temperatures of 22.4, 25.7, and 36.0 K. The spectra are shown in Figure 1. The ordinate $\alpha(v)$ is the observed absorbance divided by the absorption path length d and by the square of the density ρ in amagat units, the ratio of the actual number density to that of an ideal gas at standard temperature and pressure, viz.,

$$\alpha(v) = -\left(\frac{1}{\rho^2 d}\right) \ln\left[\frac{I_s(v)}{I_b(v)}\right], \qquad (1)$$

where $I_s(v)$ is the hydrogen gas sample spectrum and $I_b(v)$ is a background spectrum.

Measurements of the spectra were carried out using a low-temperature multireflection absorption cell, designed specifically to transmit long-wavelength radiation, coupled to a Fourier transform spectrometer with a 1.6 K bolometer detector. The optical path through the cell was set to 52 or 60 m, and spectra were obtained at a resolution of 0.24 cm^{-1}. The apparatus and experimental procedure have been described in detail by Wishnow (1993), and more briefly by Wishnow, Ozier, & Gush (1995). Here, for clarity, a few salient points will be repeated.

The cell was cooled by flowing the boil-off gas of liquid helium through a heat exchanger attached to its outer wall. The cell temperature was controlled by adjusting the gas flow rate. During an experiment, the cell was filled with the sample gas, using pressures in the range 0.5–3 atm, and then sealed. The gas density therefore remained constant despite small temperature variations of the cell (± 1 K). The density was determined to an accuracy of 1% from simultaneous temperature and pressure readings using tabulated values of the second order virial coefficients (Dymond & Smith 1980). All experiments were conducted with normal hydrogen, that is with an ortho:para ratio of 3:1. Samples of the hydrogen gas were extracted from the cell during an experiment and checked for ortho-to-para conversion using a thermal conductivity apparatus; no conversion was observed at a sensitivity level of 1%.
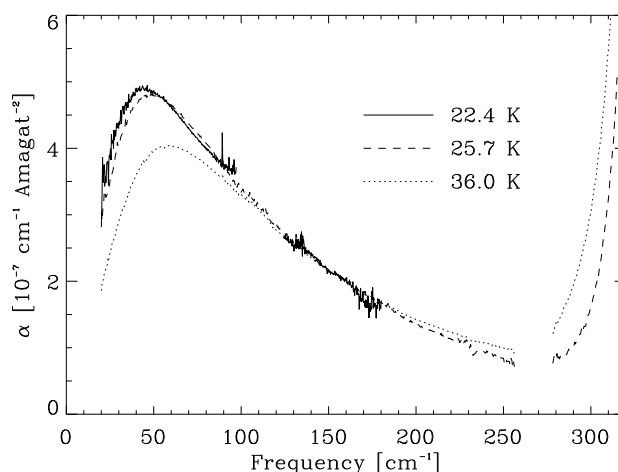

FIG. 1.—Comparison of the three measured submillimeter absorption coefficients of normal H_2: 22.4 K (*solid line*), 25.7 K (*dashed line*), 36.0 K (*dotted line*). The sharp feature at 89.2 cm^{-1} is the $R(0)$ line of HD, present in the sample in natural abundance. Amagat units are obtained by dividing the H_2 sample gas number density by Loschmidt's constant, 2.6868×10^{19} cm^{-3}.

The spectral region of interest was too broad to be studied at the required precision using a single beam splitter and filter arrangement. Measurements were conducted, during independent experimental runs, over two frequency ranges: low frequencies 20–180 cm^{-1} (LF), and high frequencies 60–320 cm^{-1} (HF). The high-frequency limit of the detector filters in both cases was deliberately chosen to exclude the peak of the $S(0)$ rotational line which has a peak intensity over 15 times that of the translational band. Preliminary studies including the $S(0)$ line showed that it interfered with a precise determination of the translational band; this may result from small nonlinearities in the bolometer response.

In Figure 1, the 22.4 K curve results from an average of LF spectra (~ 60 minutes of H_2 observations) all obtained using a gas density of 9.39 amagat. The experimental uncertainty in the gas temperature is estimated to be $+1.5/-1.0$ K. The 25.7 K curve is an average comprised of both LF and HF spectra, involving in total ~ 100 minutes of H_2 observations. The two frequency regions were combined a posteriori to give a smooth spectrum over the entire range. The final plotted result further involved the averaging of spectra weighted according to their intensity of absorption and signal-to-noise. The 36.0 K curve is obtained in the same manner where it involves ~ 160 minutes of H_2 sample observations. The range of gas densities used in the 25.7 and 36.0 K experiments was 7.3 to 23.3 amagat. The experimental uncertainty of the gas temperature associated with the average spectra is conservatively estimated to be ± 2 K.

Referring to Figure 1, the translational band is the smooth continuum with a maximum at about 50 cm^{-1}, and the sharply rising absorption near 300 cm^{-1} is the low frequency wing of the $S(0)$ rotational line. Although the weak high-frequency tail of the translational band extends to above 400 cm^{-1}, the overlap with the $S(0)$ line is small, and the translational band is clearly resolved for the first time. No sharp features in these spectra can be attributed to H_2. A few other features are visible in Figure 1. A weak sharp feature is present at 89.2 cm^{-1}, where this is the $R(0)$ line of hydrogen deuteride, present in the H_2 gas as a minute natural impurity (Wishnow, Ozier, & Gush 1992). A gap appears in the 22.4 K spectrum due to a null in the efficiency of the LF beam splitter. The 25.7 and 36.0 K curves are smoother than the 22.4 K curve as they involve averages of LF and HF spectra, higher gas densities, and more data. The gap in the spectrum near 270 cm^{-1} is due to an absorption band of a crystal quartz detector filter, and a distortion near 230 cm^{-1} is an artifact due to an absorption band of water ice.

The accuracy of the absorption coefficients reported here is estimated to be $\pm 5\%$ of the peak of the absorption curves. This error estimate is comprised of a component due to the reproducibility of spectra obtained under similar conditions, and a component due to uncertainties in the density. The reproducibility component includes a contribution due to an error in the determination of the temperature, since this results in an uncertainty in the shape and intensity of the spectrum. From theoretical spectra calculated using the method of § 3, the change in the peak intensity due to a ± 1 K change in T is $\pm 3.4\%$ at 22.4 K; $\pm 2.3\%$ at 25.7 K; and $\pm 1.6\%$ at 36.0 K.

The temperature dependence of the spectra in Figure 1 shows several interesting features. As T is lowered, the peak of the translational band becomes stronger and moves to lower frequency, while the low-frequency wing of the $S(0)$ line becomes weaker and steeper. Perhaps the most striking aspect of the temperature dependence is that between about 120 and 180 cm^{-1} the spectra at all three temperatures are indistinguishable. The curves coincide to within the narrow band of the high-frequency noise on the traces, i.e., to within 1% of the intensity at the peak (see § 4 below).

3. CALCULATED SPECTRUM

A few general remarks should be made about the sets of input data for the interaction potential and the dipole moment function used to calculate the collision-induced absorption spectra. The previously tested interaction potential of H_2–H_2, obtained by Meyer & Schaefer (1979) using quantum chemical calculations (dubbed M80), has been empirically improved (Schaefer & Köhler 1989; Schaefer 1994) especially in the attractive region; these results have been used in the calculation of the spectra discussed in this paper. Four interaction potential terms of the spherical expansion of the rigid-rotor H_2–H_2 system were empirically adapted previously, and they are now used in the close-coupled formalism (Arthurs & Dalgarno 1960) to calculate wave functions and eigenvalues of the bound dimers and partial wave expansions of scattering wave functions at relative velocities up to 6000 m s^{-1}. The isotropic V_{000} term has been refined in order to reproduce accurately the low-temperature second-order viral coefficients of para-H_2 measured by Long & Brown (1937) and Goodwin et al. (1964). This main correction of the potential has been published (Schaefer & Köhler 1989). The anisotropic terms V_{022} ($= V_{202}$) and V_{224} of the spherical expansion have been adapted to results of molecular beam magnetic resonance experiments of Verberne (1979) and Verberne & Reuss (1980, 1981) by comparing the hyperfine spectra of ortho-para and ortho-ortho H_2 dimers. These very small corrections of the potential have not yet been published.

The rigid-rotor dipole moment function has been used as published by Meyer, Borysow, & Frommhold (1989) who provided analytical fits of the spherical expansion coefficients. Previously published results of the H_2 spectrum near $S(0)$ (McKellar & Schaefer 1991) used a slightly different (preliminary and unpublished) dipole moment function, from W. Meyer (1982, private communication); this work also utilized a scaling factor for the dipole moment of 0.955. The analysis of the translational band presented here uses the newer dipole moment function and no scaling factor. It is this change in the dipole moment function that is responsible for the improved agreement between experiment and theory, as compared with that noted previously (Wishnow et al. 1995; Schaefer 1995).

The theoretical spectra are compared to their experimental counterparts in Figures 2, 3 and 4 for $T = 22.4, 25.7,$ and 36.0 K, respectively. As can be seen from Figure 3, the spectrum is dominated by the free-free component, with bound-free absorption contributing about 10% at the peak of the translational band for $T = 25.7$ K. The bound-free component was determined by assuming thermodynamical equilibrium for the dissociation of the dimers. As can be seen from Figure 3 of Schaefer (1994), the equilibrium dimerization constant is approximately 0.33×10^{-2} amagat^{-1} for normal H_2 at 25 K; this was determined from the known dimer binding energies. The translational band arises entirely from ortho-para and ortho-ortho pairs. The para-para pairs do not contribute; only ($j = 0$) para-H_2 is
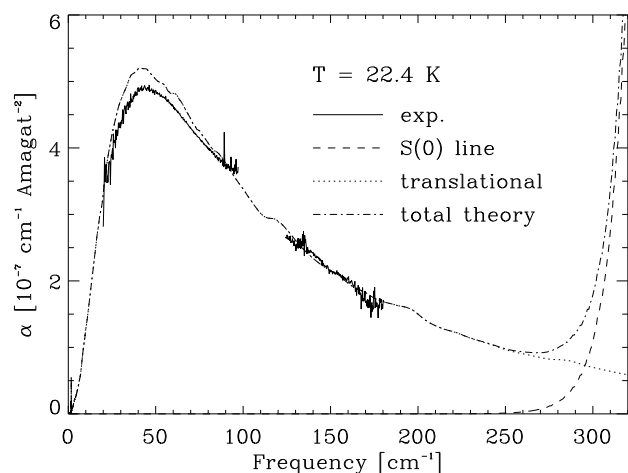
FIG. 2.—Comparison of the measured and calculated ab initio absorption coefficients for normal H_2 at 22.4 K. The experimental spectrum is shown with the solid line; the gap is due to poor performance of the beam splitter in the LF configuration, the only one used in this set of measurements. The theoretical spectrum is shown with the dot-dashed line. This is decomposed into the pure translational band (*dotted curve*) and the translation-rotation contribution S(0) (*dashed curve*). The weak, sharp line calculated near the origin arises from an ($l = 2 \leftarrow 1$) H_2 bound-resonance transition.

present at these low temperatures, and two ($j = 0$) para-H_2 molecules form only states of one parity (positive).

In discussing the labeling of the wavefunctions, it is important to recognize that each eigenfunction is a superposition of basis states with different values of l. It is, nonetheless, convenient to label each wave function by the l-value of the basis state with the largest admixture. This convention has been adopted here. All of the H_2–H_2 bound states have dominant l-basis functions with $l = 0$ or 1.

The theoretical spectra do not exhibit significant narrow features over the spectral range 20–320 cm^{-1}. Small features are visible in the calculated spectra over this frequency range, but these features are spurious, caused by the
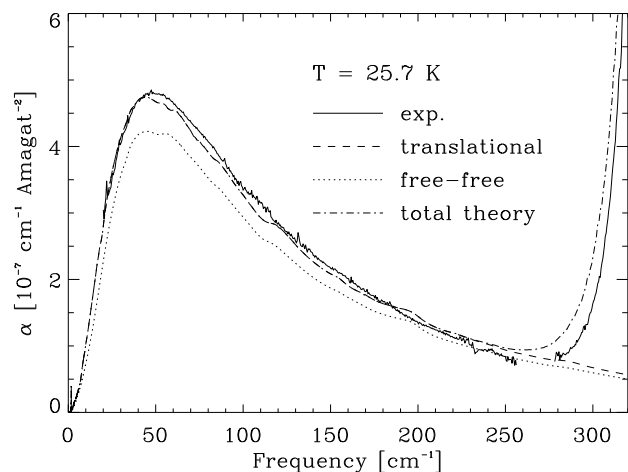
numerical treatment of the continuum wave functions. The absence of bound-bound transitions in this spectral range can be seen directly from Table 1 of Schaefer (1994), which shows that all the bound dimer states fall in an energy interval smaller than 2 cm^{-1}. This occurs in large part, because of the small magnitude of the attractive dispersion forces in the H_2–H_2 system.

The spectrum of sharp lines is further limited by the fact that the leading terms in the dipole moment expansion, denoted A_{0223} and A_{2023} by Meyer, Borysow, & Frommhold (1989), require states with $l \geq 2$. These two terms provide almost all the intensity in the spectra calculated here. These terms will contribute to bound-bound and orbiting resonance lines, but only through small admixtures of $l \geq 2$ basis components into levels dominated by $l = 0$ or 1. The very weak absorption spectrum for these narrow features for normal H_2 at 20 K has been shown in a previous paper (see Fig. 4 of Schaefer 1994). The strongest sharp features are two bound-resonance lines at 1.45 and 1.7 cm^{-1}; these are far below the lowest frequency reached in these measurements. The theory predicts two bound-free bands just below $v = 20$ cm^{-1} due to $l = 2 \leftarrow 1$ and $l = 3 \leftarrow 0$ transitions, but these do not show up as isolated features in the calculated spectra for temperatures above 20 K because the free-free absorption is too strong.

4. COMPARISON OF EXPERIMENT AND THEORY

Figures 2–4 show the excellent overall agreement between the measured and calculated hydrogen spectra. Without adjusting any parameters to fit the current data, the calculated spectrum differs from its experimental counterpart by less than the experimental error over almost the entire range measured. Four particular aspects of the comparison merit detailed discussion.

First, in Figure 2, near the intensity maximum, the calculated spectrum is higher than the measurements by about 7%, which is slightly outside the experimental error of 5%. This discrepancy is not considered to be serious. The theoretical curve has been recalculated for temperatures slightly above and slightly below the experimental mean of 22.4 K. An almost perfect match is found over the entire translational band below 220 cm^{-1} for $T = 23.4$ K, a temperature which is within the experimental uncertainty in T.

FIG. 3.—Comparison of the measured and calculated ab initio absorption coefficients for normal H_2 at 25.7 K. The experimental spectrum is shown with a solid line, and its calculated counterpart is shown with the dot-dashed line. Below 250 cm^{-1}, the latter is dominated by the pure translational band, which is shown as a dashed curve where it deviates significantly from the total. The dotted curve shows the free-free contribution to the translational band; the remaining intensity in this band arises from bound-free (and free-bound) transitions.
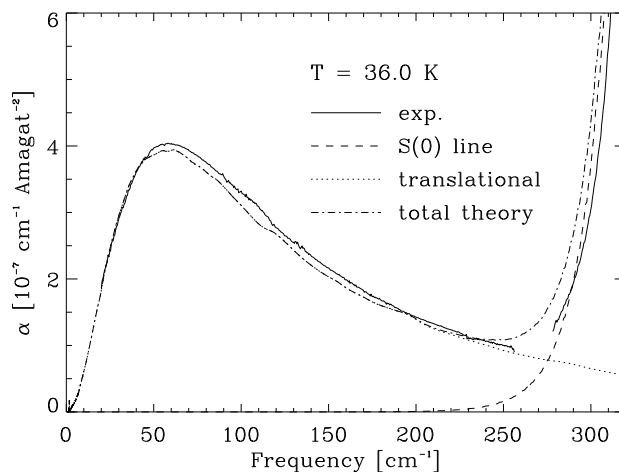

FIG. 4.—Comparison of the measured and calculated ab initio absorption coefficients for normal H_2 at 36.0 K. The four different curves are as defined in the caption of Fig. 2.

This "disagreement" illustrates the dependence of the uncertainty of the measured spectra on the error in the temperature.

Second, in both Figures 3 and 4, the calculated spectrum is higher than the measured low-frequency wing of the $S(0)$ rotational line by amounts clearly outside the quoted experimental error. The discrepancy between theory and experiment is similar to one reported by Schaefer & McKellar (1990) in a study of the $S(0)$ line of para-hydrogen at 77 K. In the current work, the experimental data may be suspect, as the relatively strong $S(0)$ line lies near the high-frequency limit of the measurements where the error is greater than in the middle of the spectral band. [Note that over this $S(0)$ region, the 36.0 K spectrum is considered more reliable than the 25.7 K spectrum, as it suffers less distortion due to a water ice feature.] To resolve this discrepancy, a new specialized experiment focused on the precise determination of the low-temperature spectrum near $S(0)$ will be required.

Third, the agreement between experiment and calculation between 120 and 180 cm^{-1} is much better than might be expected from the quoted experimental error of 5% (of the peak of the translational band). As noted in § 2, the observed spectra for all three temperatures are virtually coincident. The same is true for the corresponding theoretical curves. The insensitivity to T can be understood as follows. Bound-free transitions contribute little, so that only the free-free contributions need be considered. Their intensity is obtained from an integral over E_i of the quantity $(E_i E_f)^{-1/2}$ (E_i is the initial and E_f the final energy) times the normalized Maxwell-Boltzmann distribution of the initial energy. This distribution has a temperature dependence of the form $(T^{-1.5}) \exp(-E_i/kT)$. As T increases, each energy point contributes less so that the maximum drops in intensity. However, at any given frequency, more and more energy points with increasing initial energy contribute to the integral due to the Boltzmann factor. Between 22 and 36 K, the two effects cancel to well within the experimental error over the interval 120–180 cm^{-1}.

For this spectral range, the excellent internal agreement between the curves of Figure 1 along with the close correspondence between experiment and theory shows that several potential sources of systematic experimental errors have been properly taken into account. These errors include: drifts in detector sensitivity, definition of the zero of transmission, measurement of gas density, and ortho-para conversion.

Finally, it is of interest to compare the experimental and theoretical values of the integrated intensity of the translational band α_{1TR}. To obtain the experimental value, it was necessary to overcome the difficulty that the high frequency wing of the translational band (i.e., above 250 cm^{-1}) was not measured. A synthetic spectrum (Bachet et al. 1983) was fitted to the measurements and then used to determine α_{1TR}. The theoretical value of α_{1TR} was obtained by numerical integration of the spectra up to 400 cm^{-1}. The contribution of the small remaining tail above this limit was added by assuming exponential decrease with frequency. In units of 10^{-32} cm^5 s^{-1}, the experimental/theoretical values of α_{1TR} were 2.125/2.182 at 22.4 K; 2.007/2.052 at 25.7 K; and 1.841/1.846 at 36.0 K. The theoretically obtained integrated intensities are all slightly larger, with a mean difference of 1.7%. Since the main discrepancy in the spectra was due to the $S(0)$ line which is now excluded, this good agreement for α_{1TR} is not surprising. Because the high-frequency tail of the translational band is the same, or higher in intensity, at 36.0 K as it is at 25.7 K (as is indicated by the data in Fig. 1), the increase in α_{1TR} as T is lowered from 36 K is due entirely to absorption below about 120 cm^{-1}.

Very recently, a quantum mechanical calculation of the 36.0 K H$_2$ spectrum performed by Frommhold has been mentioned in footnote 4 of Birnbaum et al. (1996). This calculation, based on work published by Meyer, Frommhold, & Birnbaum (1989), is stated to have absorption coefficients 10%–15% less than the translational measurements presented here. However, Meyer et al. (1989) report that calculated spectra using this method match well the 77 K measurements of the $S(0)$ line by Birnbaum (1978). The primary difference between these calculations and the current work is that the former used an isotropic H$_2$–H$_2$ interaction potential, whereas the current theoretical spectra use an anisotropic potential which has been further refined as described in § 3 and by Schaefer (1994). In addition, symmetry requirements have been obeyed in the current work which could have led to minor changes in the results as well. It should be noted that the current improved calculation also gives a good match with the 77 K measurements of Birnbaum. It is because the translational band has such low intensity that the difference between the two approximation methods appears to be relatively large over this region. In fact, this consideration holds only for systems with weak anisotropic interaction potentials.

An excellent correspondence has been obtained here between measurements and ab initio quantum mechanical calculations of the H$_2$ spectrum at temperatures near 25 K. This correspondence shows in particular that the large quantum effects in the translational motion due to the low temperature and low molecular mass of the gas have been properly treated. As a result, one has confidence that the theoretical analysis, involving the H$_2$–H$_2$ interaction potential, the model of the induced dipole moment, and the computational method is valid. Furthermore, the theory can be used to accurately predict the spectrum of H$_2$ in temperature and pressure ranges beyond those accessible to laboratory measurement.

REFERENCES

Arthurs, A. M., & Dalgarno, A. 1960, Proc. R. Soc. London A, 256, 540
Batchet, G., Cohen, E. R., Dore, P., & Birnbaum, G. 1983, Canadian J. Phys., 61, 591
Birnbaum, G. 1978, J. Quant. Spectrosc. Radiat. Transfer, 19, 51
Birnbaum, G., Borysow, A., & Orton, G. S. 1996, Icarus, 123, 4
Broeils, A. 1992, Ph.D. thesis, Rijksuniv., Groningen, Netherlands
Conrath, B., et al. 1989, Science, 246, 1454

Dymond, J. H., & Smith, E. B. 1980, The Virial Coefficients of Pure Gases and Mixtures: A Critical Compilation (Oxford: Clarendon)
Frommhold, L. 1993, Collision-induced Absorption in Gases (Cambridge: Cambridge Univ. Press)
Goodwin, R. D., Diller, D. E., Roder, H. M., & Weber, I. A. 1964, J. Res. NBS, 68A, 121
Hanel, R., et al. 1986, Science, 233, 70

Long, E. A., & Brown, O. L. I. 1937, J. Am. Chem. Soc., 59, 1922
Mather, J. C., et al. 1995, *COBE* Far Infrared Absolute Spectrophotometer (FIRAS) Explanatory Supplement, *COBE* Ref. Pub. 95-C (Greenbelt, MD: NASA/GSFC)
McKellar, A. R. W., & Schaefer, J. 1991, J. Chem. Phys., 95, 3081
Meyer, W., Borysow, A., & Frommhold, L. 1989, Phys. Rev. A, 40, 6931
Meyer, W., Frommhold, L., & Birnbaum, G. 1989, Phys. Rev. A, 39, 2434
Meyer, W., & Schaefer, J. 1979, J. Chem. Phys., 70, 344
Pfenniger, D., & Combes, F. 1994, A&A, 285, 94
Pfenniger, D., Combes, F., & Martinet, L. 1994, A&A, 285, 79
Schaefer, J. 1994, A&A, 284, 1015
———. 1995, in Collision- and Interaction-induced Spectroscopy, NATO ASI Ser., ed. G. C. Tabisz & M. N. Neuman (Dordrecht: Kluwer), 485
———. 1996, Europhys. Lett., 34, 69

Schaefer, J. 1997, in progress
Schaefer, J., & Köhler, W. E. 1989, Z. Phys. D, Atoms, Molecules and Clusters, 13, 217
Schaefer, J., & McKellar, A. R. W. 1990, Z. Phys. D, Atoms, Molecules and Clusters, 15, 51; erratum 17, 231
Verberne, J. 1979, Ph.D. thesis, Katholieke Univ., Nijmegen, Netherlands
Verberne, J., & Reuss, J. 1980, Chem. Phys., 50, 137
———. 1981, Chem. Phys., 54, 189
Wishnow, E. H. 1993, Ph.D. thesis, Univ. British Columbia, Vancouver, Canada
Wishnow, E. H., Ozier, I., & Gush, H. P. 1992, ApJ, 392, L43
———. 1995, in Collision- and Interaction-induced Spectroscopy, NATO ASI Ser., ed. G. C. Tabisz & M. N. Neuman (Dordrecht: Kluwer), 495